Acta Crystallographica Section D
Biological Crystallography
ISSN 0907-4449

Spore-coat laccase CotA from *Bacillus subtilis*: crystallization and preliminary X-ray characterization by the MAD method

Francisco J. Enguita,[a] Pedro M. Matias,[a] Lígia O. Martins,[a,b] Diana Plácido,[a] Adriano O. Henriques[a] and Maria Arménia Carrondo[a]*

[a]Instituto de Tecnologia Química e Biológica, Universidade Nova de Lisboa, 2781-901 Oeiras, Portugal, and [b]Universidade Lusófona de Humanidades e Tecnologias, Departamento de Engenharias e Tecnologias, Av. do Campo Grande 376, 1749-024 Lisboa, Portugal

Correspondence e-mail: carrondo@itqb.unl.pt

Received 25 April 2002
Accepted 1 July 2002

Bacterial endospores are highly resistant structures that allow survival for long periods of time in adverse environments. The spore-forming Gram-positive bacterium *Bacillus subtilis* synthesizes a coat around the endospore during development composed of several assembled polypeptides. The role of these components of the spore coat remains unclear; however, some of them appear to be enzymes possibly involved in the assembly process or in the final properties of the spore. The outer spore-coat protein CotA is a 65 kDa polypeptide showing a high degree of sequence similarity with copper-dependent oxidases, including fungal and plant laccases, ascorbate oxidase and CueO from *Escherichia coli*. CotA has been recently characterized as a copper-dependent laccase. Unlike previously reported laccases, CotA shows increased thermostability. Here, the crystallization of a recombinant CotA protein produced in *E. coli* and the preliminary characterization of the crystals is reported. Structure solution by the MAD method at the copper *K* edge is also reported.

1. Introduction

Endospores formed by the Gram-positive soil bacterium *B. subtilis* are encased in a protein coat formed by the ordered synthesis and assembly of over 30 polypeptides ranging in size from ~5 to 65 kDa. The coat confers protection against bactericidal enzymes and harsh chemicals and also allows the spore to monitor its environment and to promptly initiate germination in response to appropriate stimuli (Driks, 1999; Henriques & Moran, 2000). Assembly of the multiprotein coat structure appears to rely on specific protein–protein interactions, which may be enforced by post-translational modification events such as protein cross-linking, proteolysis and glycosylation (Driks, 1999; Henriques & Moran, 2000). Little is known about the structure or function of individual coat proteins, but some components appear to be enzymes with possible roles in the assembly process or in the final spore properties. For example, a manganese catalase associates with the inner coat layers (Henriques *et al.*, 1995; Seyler *et al.*, 1997), whereas a transglutaminase associates with the outer coat layers (Kobayashi *et al.*, 1996; Suzuki *et al.*, 2000). Another enzyme that occurs at the spore outer layer is CotA (Donovan *et al.*, 1987; Hullo *et al.*, 2001; Martins *et al.*, 2002). The 65 kDa CotA has recently been shown to have copper-dependent laccase activity (Hullo *et al.*, 2001; Martins *et al.*, 2002). Unlike other well characterized laccases, CotA is remarkably resistant to thermal denaturation (Martins *et al.*, 2002). In an effort to begin to understand the process of assembly of the endospore coat structure, we have initiated the structural characterization of selected coat components. Here, we report on the crystallization and preliminary X-ray characterization of *B. subtilis* CotA, which was purified from an over-producing *E. coli* host.

Laccases are oxidases able to act over a wide variety of substrates, including phenolic compounds, and therefore have potential biotechnological applications. Laccase (EC 1.10.3.2) belongs to the blue multi-copper oxidase family, which also includes ascorbate oxidase (EC 1.10.3.3), ceruloplasmin (EC 1.16.3.1), manganese oxidases and other enzymes, such as CueO from *E. coli* (Gray *et al.*, 2000; Roberts *et al.*, 2002). They contain two distinct types of copper centres: a mononuclear exposed type 1 centre, responsible for monoelectronic oxidations of substrates, and a trinuclear internal copper centre, which stores and transfers four electrons to molecular oxygen, coupling the substrate oxidation with the four-electron reduction of a single dioxygen molecule (Ducros *et al.*, 1998). The trinuclear copper centre is composed of two subcentres: a type 2 copper centre and a type 3 copper centre. The type 3 copper centre is binuclear, with Cu atoms antiferromagnetically coupled by a hydroxide ligand (Karlin *et al.*, 1998). The mechanism for electron transfer

between the mononuclear and trinuclear copper centres is still not well understood; however, several models have been proposed based on spectroscopic studies (Messerschmidt *et al.*, 1993).

2. Materials, methods and results

2.1. Overproduction and purification of CotA

The *cotA* gene was amplified by PCR and the 1733 bp PCR product was cloned in the vector pET21a(+) (Novagen) to yield pLOM10. Introduction of pLOM10 into the *E. coli* strain Tuner (DE3) (Novagen) produced strain AH3517, able to overproduce the CotA protein under the control of the T7*lac* promoter (Martins *et al.*, 2002). Strain AH3517 was grown in LB medium supplemented with 0.25 m*M* $CuCl_2$ at 303 K. Growth was followed until the mid-log phase, at which point CotA overproduction was induced by addition of 1 m*M* IPTG. Cells were harvested by centrifugation after 4 h and cell sediment was suspended in 20 m*M* Tris–HCl pH 7.6 containing DNase I (10 µg ml^{-1} extract), 5 m*M* $MgCl_2$ and a mixture of protease inhibitors. Cells were disrupted in a French pressure cell at 131 MPa, followed by ultracentrifugation (40 000*g*, 1 h, 277 K) to remove cell debris and membranes. The resulting soluble extract was loaded onto an ion-exchange SP-Sepharose column equilibrated with 20 m*M* Tris–HCl pH 7.6. Elution was carried out with an NaCl gradient. Fractions containing laccase-like activity were pooled and concentrated by ultrafiltration. The resulting sample was applied to a Mono S HR5/5 column (Amersham Pharmacia Biotech). Elution was carried out with an NaCl gradient and active fractions were pooled and desalted. After boiling for 10 min in loading dye, a single protein band with molecular weight 65 kDa was revealed by SDS–PAGE. All purification steps were carried out at room temperature in a fast protein liquid-chromatography system (Åkta FPLC, Amersham Pharmacia Biotech).

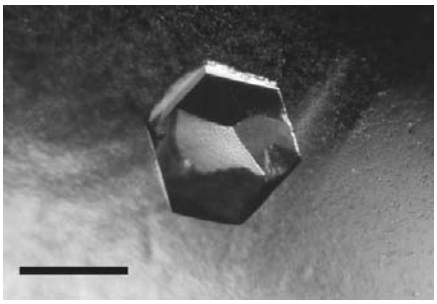

Figure 1
Microphotography of CotA crystals obtained by the sitting-drop vapour-diffusion method. Crystals showed the blue colour characteristic of the presence of type I copper centres within the protein structure. The solid bar corresponds to 0.3 mm.

Table 1
Data-collection statistics of CotA crystals.

Values in parentheses are for the outer shell.

	High resolution	Cu peak	Cu inflection	Cu remote
Place of data collection	ESRF, Grenoble, France	EMBL, Hamburg, Germany		
Data-collection beamline	ID14-2	BW7A		
Wavelength (Å)/Energy (eV)	0.933	1.3768/9005.2	1.3791/8990.2	1.2397/10000.4
Space group	$P3_121$			
Unit-cell parameters (Å, °)	$a = b = 101.8$, $c = 136.1$, $\alpha = \beta = 90.0$, $\gamma = 120.0$	$a = b = 101.6$, $c = 135.7$, $\alpha = \beta = 90.0$, $\gamma = 120.0$		
Resolution limits (Å)	50.0–1.70 (1.73–1.70)	50.0–2.50 (2.56–2.40)	50.0–2.60 (2.66–2.60)	50.0–2.35 (2.40–2.35)
Total No. of reflections	835984	246306	99035	209288
No. of unique reflections	90124	32334	25388	36568
Average redundancy	9.28	12.81	5.41	7.40
Completeness (%)	99.9 (100.0)	100.0 (100.0)	99.8 (97.0)	99.5 (98.5)
$I/\sigma(I)$	16.04 (2.50)	11.88 (2.10)	13.75 (2.34)	13.36 (2.25)
R_{merge}† (%)	5.1 (29.1)	5.6 (37.0)	4.7 (27.2)	5.0 (34.4)
$R_{r.i.m.}$‡ (%) (outer shell)	5.5 (30.8)	6.0 (38.5)	5.5 (31.8)	5.5 (37.9)
$R_{p.i.m.}$‡ (%) (outer shell)	1.8 (10.0)	2.1 (13.9)	2.8 (16.3)	2.3 (15.7)
R_{anom}§ (%)	—	4.1	4.0	3.5

† $R_{merge} = \sum_{hkl}\sum_i |I_i(hkl) - \overline{I(hkl)}|/\sum_{hkl}\sum_i I_i(hkl)$. ‡ Defined in Weiss (2001). § $R_{anom} = \sum |(I^+) - (I^-)|/\sum |(I^+) + (I^-)|$, where (I^+) and (I^-) denote the mean intensity values of each mate in a Bijvoet pair.

2.2. Crystallization

Crystallization trials were set up in Linbro multiwell tissue-culture plates using the sitting-drop vapour-diffusion method. Preliminary crystallization conditions were established using the Hampton Research Crystal Screening kits I and II at 295 K, followed by a refinement of the conditions through variation of protein concentration, precipitant, pH, drop volume and additives.

Optimal conditions for CotA crystal growth were obtained using 4 µl drops containing 10–15 mg ml^{-1} purified CotA protein and a reservoir solution containing 100 m*M* sodium citrate buffer pH 5.5, 15% glycerol, 12–15% 2-propanol and 12–15% PEG 4K. It typically took 2–7 d to obtain crystals of dimensions suitable for X-ray studies (Fig. 1). CotA crystals belong to space group $P3_121$, with unit-cell parameters $a = b = 101.8$, $c = 136.1$ Å, $\alpha = \beta = 90$, $\gamma = 120°$, a unit-cell volume of 1.21×10^6 $Å^3$ and one protein molecule per asymmetric unit.

2.3. X-ray measurements and data processing

CotA crystals were harvested from the mother liquor and flash-frozen for data collection in a nitrogen-gas stream at 110 K. Prior to flash-freezing, crystals were soaked for 20 s in a cryoprotectant solution containing 100 m*M* sodium citrate buffer pH 5.5, 25% glycerol, 12% 2-propanol and 12% PEG 4K.

High-resolution X-ray diffraction data were collected at the ESRF, Grenoble, France (beamline ID14-2) using an ADSC Quantum 4 CCD detector at a resolution limit of 1.7 Å. X-ray data were processed with *MOSFLM* (Leslie, 1992) and scaled with *SCALA* (Collaborative Computational Project, Number 4). Details of data processing and statistics are given in Table 1. The Matthews coefficient (Matthews, 1968) for CotA crystals was calculated on the basis of one 65 kDa molecule per asymmetric unit, giving a value of 2.9 $Å^3$ Da^{-1}, which corresponds to an estimated solvent content of 55%.

Because CotA crystals contained copper, we decided to use this atom as an anomalous scatterer for structure determination using the multiwavelength anomalous dispersion (MAD) method. For this purpose, a MAD experiment at the copper edge was performed at EMBL, Hamburg, Germany. X-ray data were collected at EMBL beamline BW7A using a MAR 165 CCD detector. Based on the X-ray absorption spectrum of CotA crystals, two energies were chosen near the *K* absorption edge of the Cu atom: 9.005 keV (λ = 1.3768 Å, peak) and 8.990 keV (λ = 1.379 Å, point of inflection). The third energy was selected at 10.00 keV (λ = 1.2397 Å) as a high-energy remote point. The crystal diffracted to a maximum resolution of 2.35 Å at the high-energy remote wavelength. The three data sets

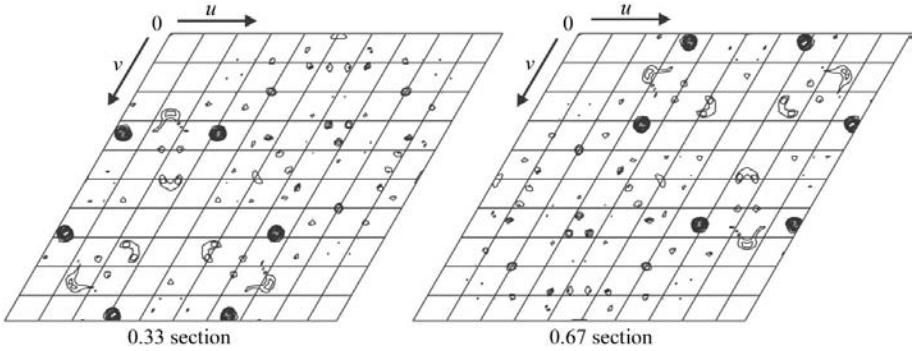

Figure 2
Anomalous difference Patterson map at 4.0 Å resolution calculated using the data set collected at the copper peak. Two Harker sections on the z plane are shown, with contour levels starting at 1.5σ and increasing in steps of 0.5σ.

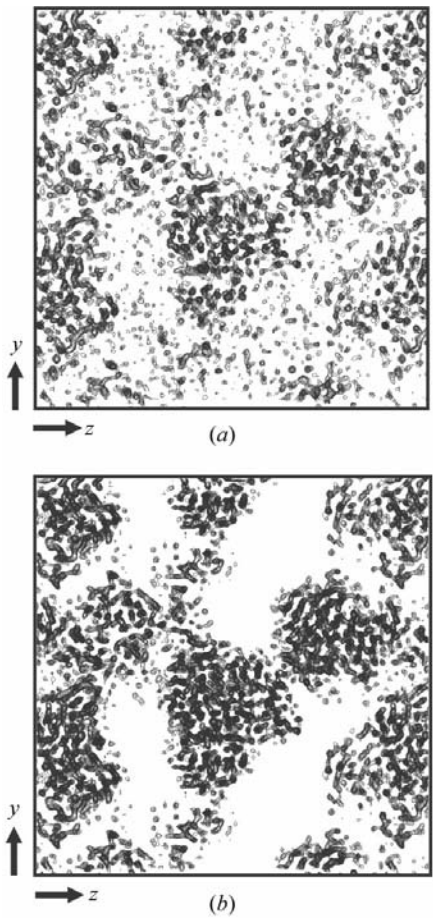

Figure 3
Superposition of 15 electron-density map sections from a total of 121 calculated (*a*) using the initial MAD phases and (*b*) using the density modified with *RESOLVE* (Terwilliger, 2001) to a resolution of 3.0 Å. Contours were drawn at 0.5σ unit intervals starting from 1.5σ. Plots were prepared with *NPO* and *XPLOT84_DRIVER* from the *CCP*4 suite (Collaborative Computational Project, Number 4, 1994).

corresponding to the MAD experiment were processed with *MOSFLM* (Leslie, 1992) and scaled individually with *SCALA* (Collaborative Computational Project, Number 4, 1994).

2.4. Structure determination by MAD phasing

For structure solution, the MAD method was used (see Table 1 for data-collection statistics). Peak, point of inflection and high-energy remote data sets were scaled together with *SCALEIT* from the *CCP*4 suite (Collaborative Computational Project, Number 4, 1994). *SOLVE* version 1.18 (Terwilliger & Berendzen, 1999) was used for interpretation of anomalous Patterson maps (Fig. 2), localization of the Cu atoms within the protein structure and refinement of their positional parameters and phasing. The best solution of automated Patterson interpretation clearly determined the position of two of the four expected Cu atoms per protein molecule, one of them partially occupied, with a mean figure of merit of 0.39 and an overall Z score of 10.1. Refined positional parameters for these two Cu atoms were used to calculate initial phases and electron-density maps, which showed a clear distinction between protein and solvent regions, indicating that the Patterson solution was correct. The initial phases (Fig. 3*a*) were further improved by density modification (Fig. 3*b*) with *RESOLVE* (Terwilliger, 2001), with a calculated final figure of merit of 0.7.

3. Discussion

The crystallization conditions described for CotA protein included the presence of 2-propanol. At concentrations between 12 and 15%, this compound has been shown to be a crucial factor in crystal quality for X-ray diffraction.

If CotA crystals were allowed to grow for too long, they lost their blue colour after approximately 7–10 d in the mother liquor. This may be owing to the loss of Cu atoms from the type 1 centre, which is responsible for the characteristic blue colour in multi-copper oxidases. For this reason, crystal harvesting was performed 48 h after the crystals had reached a maximum size of 0.2–0.5 mm in the largest dimension.

After performing the MAD experiment, analysis of Bijvoet and dispersive Patterson maps clearly showed the presence of an anomalous scatterer signal (Fig. 2). The strongest peaks in Harker sections arose from cross vectors between two Cu atoms. Automated interpretation of the anomalous difference Patterson map using *SOLVE* (Terwilliger & Berendzen, 1999) determined the coordinates of these two Cu atoms within the structure, which corresponded to the exposed mononuclear copper centre and to one of the atoms of the internal trinuclear centre. This Cu atom showed partial occupancy, probably because of the low copper content of the initial protein sample (Martins *et al.*, 2002). After heavy-atom positional parameters refinement and initial phases calculation and in spite of the poor phasing statistics, calculated maps unambiguously showed the molecular boundary within the asymmetric unit after map improvement and solvent flipping (Fig. 3*b*). Phase extension of the initial phases to 1.7 Å with *DM* (Cowtan, 1994) using the maximum-resolution data set available allowed clear visualization of all the ligands of the mononuclear copper centre. However, the definition of the electron density within the trinuclear copper cluster region was not suitable for manual density interpretation at this stage. Model building and structure refinement are presently under way.

Access to the EMBL Hamburg Facility is supported by the European Commission 'Access to Research Infrastructure Action of the Improving Human Potential' programme (contract No. HPRI-1999-CT-00017). The authors would like to thank the ESRF and ISBG staff for support during the use of beamline ID-14-2, Dr E. Pohl of EMBL, Hamburg for excellent technical assistance during the data collection and structure solution and Dr C. Soares of ITQB for helpful discussions during the elaboration of this manuscript. F. J. Enguita was supported by an EMBO long-term fellowship followed by a PRAXIS XXI post-doctoral fellowship (FCT, Ministério de Ciência e Tecnologia, Portugal).

References

Collaborative Computational Project, Number 4 (1994). *Acta Cryst.* D**50**, 760–763.
Cowtan, K. (1994). *Jnt CCP4/ESF–EACBM Newsl. Protein Crystallogr.* **31**, 34–38.

Donovan, W., Zheng, L. B., Sandman, K. & Losick, R. (1987). *J. Mol. Biol.* **196**, 1–10.
Driks, A. (1999). *Microbiol. Mol. Biol. Rev.* **63**, 1–20.
Ducros, V., Brzozowski, A. M., Wilson, K. S., Brown, S. H., Østergaard, P., Schneider, P., Yaver, D. S., Pedersen, A. H. & Davies, G. J. (1998). *Nature Struct. Biol.* **5**, 310–316.
Gray, H. B., Malmstrom, B. G. & Williams, R. J. P. (2000). *J. Biol. Inorg. Chem.* **5**, 551–559.
Henriques, A. O., Beall, B. W., Roland, K. & Moran, C. P. Jr (1995). *J. Bacteriol.* **177**, 3394–3406.
Henriques, A. O. & Moran, C. P. Jr (2000). *Methods*, **20**, 95–110.
Hullo, M.-F., Moszer, I., Danchin, A. & Martin-Verstraete, I. (2001). *J. Bacteriol.* **183**, 5426–5430.
Karlin, K. D., Zhu, Z.-Y. & Karlin, S. (1998). *J. Biol. Inorg. Chem.* **3**, 172–178.
Kobayashi, K., Kumazawa, Y., Miwa, K. & Yamanaka, S. (1996). *FEMS Microbiol. Lett.* **144**, 157–160.
Leslie, A. G. W. (1992). *Crystallographic Computing 5. From Chemistry to Biology*, edited by D. Moras, A. D. Podjarny & J. C. Thierry. Oxford University Press.
Martins, L. O., Soares, C. M., Pereira, M. M., Teixeira, M., Jones, G. H. & Henriques, A. O. (2002). *J. Biol. Chem.* **277**, 18849–18859.
Matthews, B. W. (1968). *J. Mol. Biol.* **33**, 491–497.
Messerschmidt, A., Luecke, H. & Huber, R. (1993). *J. Mol. Biol.* **230**, 997–1014.
Roberts, S. A., Weichsel, A., Grass, G., Thakali, K., Hazzard, J. T., Tollin, G., Rensing, C. & Montfort, W. R. (2002). *Proc. Natl Acad. Sci. USA*, **99**, 2766–2771.
Seyler, R., Henriques, A. O., Ozin, A. & Moran, C. P. Jr (1997). *Mol. Microbiol.* **25**, 955–966.
Suzuki, S., Izawa, Y., Kobayashi, K., Eto, Y., Yamanaka, S., Kubota, K. & Yokozeki, K. (2000). *Biosci. Biotechnol. Biochem.* **64**, 2344–51.
Terwilliger, T. C. (2001). *Acta Cryst.* D**57**, 1755–1762.
Terwilliger, T. C. & Berendzen, J. (1999). *Acta Cryst.* D**55**, 849–861.
Weiss, M. S. (2001). *J. Appl. Cryst.* **34**, 130–135.